On the ferroelastic phase transition in $LiKSO_4$: Brillouin scattering studies from 140 to 300 K and Landau theory modelling

1989 J. Phys.: Condens. Matter 1 5965

(http://iopscience.iop.org/0953-8984/1/34/013)

J. Phys.: Condens. Matter **1** (1989) 5965–5980. Printed in the UK

On the ferroelastic phase transition in $LiKSO_4$: Brillouin scattering studies from 140 to 300 K and Landau theory modelling

B Mróz†, J A Tuszyński‡, H Kiefte§ and M J Clouter§

† The Institute of Physics, A Mickiewicz University, Grunwaldzka 6, 60-780 Poznań, Poland

‡ Department of Physics, The University of Alberta, Edmonton, Alberta, Canada, T6G 2J1

§ Department of Physics, Memorial University of Newfoundland, St John's, Newfoundland, Canada, A1B 3X7

Received 20 December 1988

Abstract. In this paper we report on the results of Brillouin scattering studies of single crystals of ferroelastic $LiKSO_4$ in the range of temperatures from 140 to 300 K. We have measured all the non-zero second-order elastic constants and found them to be essentially temperature-independent except for c_{66}. The interesting hysteretic temperature dependence of c_{66}, its incomplete softening at the transition temperature and other physical properties of $LiKSO_4$ previously reported have motivated us to re-examine and extend the theoretical models adopted earlier. A Landau expansion of the free energy involved strain components including spontaneous strain, polarisation and both order parameters for the two neighbouring transitions around 190 and 250 K. As a result of this analysis we have obtained good qualitative agreement with the reported experimental data.

1. Introduction

In recent years $LiKSO_4$ has been the subject of numerous experimental investigations involving a very large variety of experimental techniques, such as thermal expansion measurements [4, 10, 19, 39, 43], x-ray studies [46, 47], dielectric, pyroelectric and piezoelectric investigations [12, 18, 36], direct microscopic observations [14], electron paramagnetic resonance [20, 25, 33, 37], and nuclear magnetic resonance analyses [34], ferroelastic [13] and polarisation [21] studies, birefringence and optical measurements [26], calorimetric investigations [1] and several Brillouin [3, 16, 22, 23, 38, 48], Raman [7, 8, 18, 22, 23, 24, 44] and neutron scattering [5, 6, 9] studies. The composite picture that emerges based on the results of these experiments is rather confusing since many of the individual experiments are mutually conflicting and sometimes irreproducible. It is quite common to observe strong dependence of the results on the history of the sample and on the way in which it has been prepared. Moreover, time dependence and hysteretic behaviour are also quite noticeable. Various techniques are able to detect only some of the phase transitions that $LiKSO_4$ undergoes and, even when they are detected, both the symmetries of the phases involved and the values of the transition temperatures are often disputed. The sequence of phase transitions taking place in $LiKSO_4$ may be represented schematically as

$$\text{Melt} \underset{T_m}{\rightarrow} \text{PI} \underset{T_1}{\rightarrow} \text{PII} \underset{T_2}{\rightarrow} \text{PIII} \underset{T_3}{\rightarrow} \text{PIV} \underset{T_4}{\rightarrow} \text{PV} \underset{T_5}{\rightarrow} \text{PVI} \underset{T_6}{\rightarrow} \text{PVIIA} \underset{T_7}{\rightarrow} \text{PVIIB} \underset{T_8}{\rightarrow} \text{PVIII} \qquad (1)$$

0953-8984/89/345965 + 16 $02.50

Table 1. The values of transition temperatures for $LiKSO_4$ according to the sources of reference.

Transition temperature	Value (K)
T_m	998 [14], 1008 [5]
T_1	940 [5], 948 [14]
T_2	695 [43], 700 [5], 708 [4, 19, 39], 711 [14], 718 [4], 720 [44]
T_3	333 [14]
T_4	190–255 [10], 201–242 [7, 8], 205–250 [9], 226 [20], 240 [5], 240–290 [18], 245 [14], 250 [12, 26, 36], 250–265 [23], 253 [25], 265 [22]
T_5	160–192 [18], 178 [43], 180–187 [10], 181–186 [20], 183 [25], 189 [5], 189–190 [9], 190 [12, 14, 18, 22, 26, 36], 190–200 [23]
T_6	74 [14], 135–138 [9], 174 [20]
T_7	53 [14], 83 [20]
T_8	20–30 [18], 38 [5, 14]

and the values of the transition temperatures have been summarised in table 1 according to the sources of reference. Table 2 lists the properties of the phases involved according to the sources of reference. At this stage it does not appear possible to determine conclusively the symmetries of the sequence of phases listed in table 2. The two ferroelastic phases PV and PVI are at the centre of this controversy.

The room-temperature crystal structure of $LiKSO_4$ is characterised by having two molecules per unit cell and by the corner sharing of two kinds of tetrahedra: LiO_4 and SO_4. The framework of these tetrahedra encloses cavities occupied by K ions. The pattern of the sharing of the corners is tridymite-like (Pm3); S and Li ions occupy alternate tetrahedra and every O ion has one Li neighbour and one S neighbour. This structure gives rise to polar properties of the crystal. The 'average' room-temperature structure of $LiKSO_4$ has been demonstrated in figure 1. The space group of the PIV phase appears to be $P6_3$ while the main candidates for the PV phase are $P31c$ and $P6_3mc$. The most likely realisation of the PVI phase is $Cmc2_1$. Following Tomaszewski and Lukaszewicz [46] and Bansal *et al* [7] we have schematically illustrated the relative orientations of the SO_4 tetrahedra in these four structures, which is shown in figure 2.

The results of our experiments are consistent with the assumption that the room-temperature hexagonal structure ($P6_3$), on lowering the temperature, undergoes a distortion of its SO_4 tetrahedra leading to a $P6_3mc$ structure with its top oxygen locations randomly distributed among the three possibilities numbered 1, 2 and 3 in figure 2. These three possibilities translate themselves into three ferroelastic domains as shown in figure 2(*e*). Lowering the temperature further appears to remove this degeneracy and to create order in the oxygen positions. This then would lead to the $Cmc2_1$ space group. Both the transitions at T_4 and T_5 are of first order and as such involve thermal hystereses. Consequently, that might account for the differences in the observed transition temperatures. Furthermore, since T_4 and T_5 are relatively close, one may expect to see the coexistence of various combinations of the three phases involved. That might be easily misinterpreted as an incommensurate structure. Moreover the possible presence of domains, defects, heterogeneities and impurities complicates the analysis even more. Finally, it should be emphasised that the negligible latent heats of the two first-order transitions [14] mean that there are very small energy differences between the various phases, and this may also explain some problems related to the irreproducibility of certain results and time-dependent effects. Recently, Brillouin and Raman scattering

Table 2. Properties of the various phases of $LiKSO_4$ according to the sources of reference.

Phase	Lattice type	Point group	Space group	Elastic properties	Electric properties
PI	Hexagonal [5, 14]	6/mm [7, 29]			
PII	Orthorhombic [5, 14, 29, 44, 48]	mmm [29]		Ferroelastic [5, 29]	Polar but not ferroelectric [4]
PIII	Hexagonal [14, 48]				
PIV	Hexagonal [11]	6 [7, 14, 22, 43]	$P6_3$ [10, 27, 42]		
PV	Hexagonal [10, 14]	6mm [5, 10, 14]	$P6_3mc$ [10, 14]	Ferroelastic [5]	Improper ferroelectric [21]
	Trigonal [7]	3m [7, 9, 33]	P31*c* [7, 33] P31*c* or $P6_3mc$ [22] Coexistence of $P6_3mc$ and $P6_3$ [10] Coexistence of $P6_3$ and P31*c* [9]		
	Incommensurate [20, 25]	3m or incommensurate [18]			
	Not incommensurate [22] Coexistence of hexagonal and triclinic [23]	2 [26]			
PVI	Orthorhombic [10, 14, 22] Pseudo-orthorhombic [9] Trigonal [7] Hexagonal [20] Not hexagonal [18] Not triclinic [5] Not monoclinic [5]	mm2 [5, 10, 14, 22]	$Cmc2_1$ [10, 14, 22] Coexistence of $Cmc2_1$, $P6_3mc$ and $P6_3$ [10] P31*c* [7] Not $Cmc2_1$ [9]	Ferroelastic [5, 12, 22, 36]	Improper ferroelastic [21]
	Distorted triclinic [48]	1 [26]			
	Commensurate [20]	2 [6]			
PVIIB	Incommensurate [20]				
PVIII	Orthorhombic [5] Hexagonal [20]			Ferroelastic [5]	

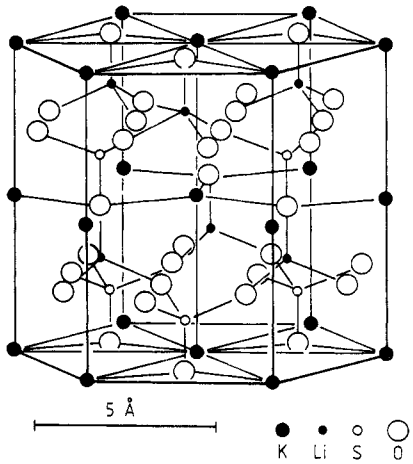

Figure 1. The 'average' room-temperature structure of $LiKSO_4$ following Bradley [11].

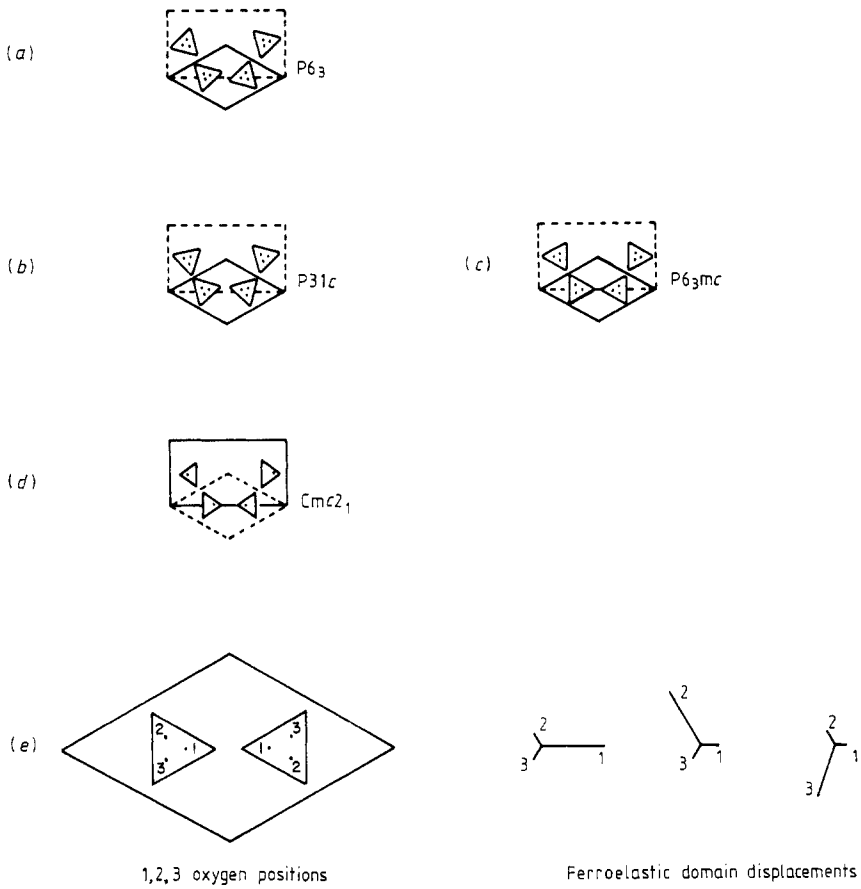

Figure 2. Relative orientations of the SO_4 tetrahedra in the space groups (*a*) $P6_3$, (*b*) P31*c*, (*c*) $P6_3mc$ and (*d*) $Cmc2_1$, and (*e*) the explanation of the numbering of the top oxygens displaced from the central position [49], which is related to the three possible ferroelastic domains of $P6_3mc$.

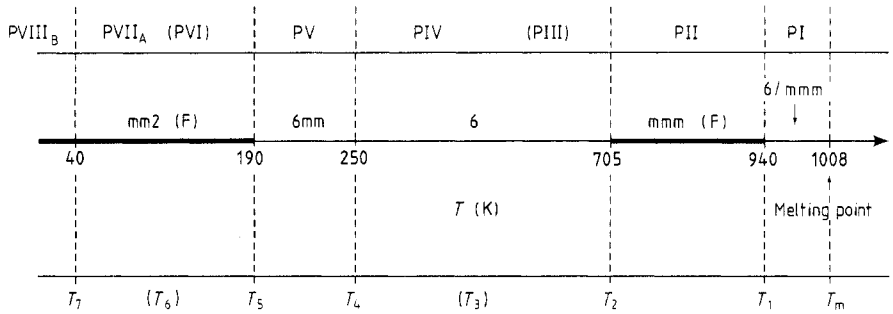

Figure 3. The sequence of structural phase transitions of $LiKSO_4$ in the crystal state adopted in the present paper.

experiments involving samples under uniaxial stress [22] demonstrated the existence of both abrupt and progressive transformations and were interpreted as resulting from the presence of local defects and heterogeneities.

The present experiment has been concerned with the ferroelastic properties of $LiKSO_4$ in the range from 140 to 300 K. It is now believed that $LiKSO_4$ undergoes two ferroelastic phase transitions from the hexagonal to the orthorhombic system: (i) from the 6/mmm to the mmm point group at about 940 K, and (ii) from the 6mm to the mm2 point group at about 190 K [28, 29, 36]. The ferroelastic character of these transitions was demonstrated by direct observation of the domain structure. Three types of domain walls inclined at an angle of 120° were observed in both phases. It was possible to reorient the domain structure under the action of an appropriate mechanical stress and this allowed for determination of stress–strain hysteresis loops in the low-temperature ferroelastic phase [36]. These results, together with the results of x-ray studies [46, 47] and recent investigations of the $LiKSO_4$ crystal using neutron scattering (time-of-flight, TOF) techniques [5], lead to the sequence of phase transitions accepted for the purpose of this paper as shown in figure 3. The diagram does not contain information concerning either the differences of the temperature dependence of its physical properties between cooling and heating [33, 36], the behaviour in the coexistence region as observed in the course of x-ray studies (see figure 7 of [46]) or the influence of the sample's thermal history [9, 14]. It is these considerations which may, in fact, explain the seemingly contradictory results of different experiments concerning the symmetries of various phases below room temperature, as discussed earlier.

Only a few papers concerning Brillouin scattering studies of the $LiKSO_4$ crystal have been published to date. The results of Drozdowski *et al* [16], obtained in the temperature range from 300 to 360 K, were discussed by Pimeta *et al* [38]. Young *et al* [48] reported on temperature studies of the Brillouin mode related to the c_{11} elastic constants in the vicinity of the phase transitions at about 708 K. Finally, the only results for the low-temperature phases of $LiKSO_4$ are presented by Ganot *et al* [23] and An *et al* [3]. Ganot *et al* investigated the temperature dependence of the two longitudinal modes corresponding to the c_{11} and c_{33} elastic constants and, additionally, An *et al* reported an anomalous temperature behaviour of the mode corresponding to the c_{66} elastic constant. In the present paper we report on Brillouin scattering studies of the $LiKSO_4$ crystal in the temperature range from 140 to 300 K. Measurements of the temperature dependence of the longitudinal and transverse Brillouin modes have allowed us to calculate all the non-zero components of the elastic stiffness tensor for the hexagonal phases 6 and 6mm.

The results of the Brillouin scattering experiment provide a basis for developing a theoretical description of the ferroelastic phase transition [17, 35]. An *et al* [3] outlined

a Landau model for the 6 → 6mm transition. Zeks *et al* [49] proposed the first, and to the best of our knowledge the only, theoretical model for the 6mm → mm2 transition of $LiKSO_4$. The results of their studies based on Landau theory lead to the conclusion that the transition is always of first order. In § 3 we expand on these two types of calculations and provide a modified theoretical description valid around both transition temperatures which appears to be in good qualitative agreement with experiment.

2. Experimental procedure and results

The colourless single crystals of $LiKSO_4$ were grown isothermally at 315 K from aqueous solution. The samples were prepared in the form of cubes ($5 \times 5 \times 5\ mm^3$) with four different orientations. We measured the sound velocities propagating along the crystallographic axes and the bisectors of the angles between these axes.

The Brillouin spectrometer and cryostat used in this experiment have been described by Ahmad *et al* [2]. The incident light, which was polarised perpendicularly to the scattering plane, was provided by a stabilised single-mode argon-ion laser (Coherent Radiation 52) operating at $\lambda = 514.5$ nm. Light scattered at 90° to the incident beam was analysed using a piezoelectrically scanned, triple-pass Fabry–Perot interferometer (Burleigh RC-110) with a free spectral range (FSR) of 25.03 GHz. The finesse was 50 and the measured contrast ratio was about 10^6. Sound velocities v were deduced from the measured frequency shifts $\Delta\nu$ using the Brillouin equation, which in the case of the 90° scattering geometry takes the form

$$v = \lambda \Delta \nu (n_i^2 + n_s^2)^{-1/2} \tag{2}$$

where λ is the wavelength of the incident light, n_i and n_s are the refractive indices for the incident and scattered light, respectively.

The sound velocities v of the three acoustic waves propagating in the direction $\boldsymbol{Q}$ can be determined from the solution of the equation of motion [31], which is given by

$$|c_{ijkl} q_j q_k - \rho v^2 \delta_{il}| = 0. \tag{3}$$

Here q_j, q_k are the direction cosines of $\boldsymbol{Q}$, ρ is the density of the crystal, c_{ijkl} are the elastic stiffness components and δ_{il} is the Kronecker delta. In order to compare our results with those obtained at 300 K by Pimeta *et al* [38], we utilise the values of the refractive indices and the density presented in their paper ($n_x = n_y = 1.4729$, $n_z = 1.4732$, $\rho = 2.383\ g\ cm^{-3}$). Following Tomaszewski and Lukaszewicz [46] the change of volume of the elementary cell at the transition temperature is less than 2%. Consequently, when calculating the elastic constants we have neglected the temperature dependence of the crystal's density and, what is related to it, the temperature dependence of the refractive indices. This is a standard practice in Brillouin scattering studies, expecially for crystals with small changes of dielectric permittivity. Notwithstanding the uncertainties concerning the low-temperature phases of $LiKSO_4$, we consider the ferroelastic phase transition of this crystal to be 6mm → mm2. Table 3 contains expressions of ρv^2 as a function of elastic constants in the hexagonal (6mm) and orthorhombic (mm2) phases [5, 28, 29, 36, 46]. Since hexagonal symmetry requires $x = y$, the solution of equation (3) gives the same sets of elastic constants for the para-elastic phase for phonons [100], [010], [110] and [011], [101]. We have determined the temperature dependence of the six Brillouin modes (γ_i, $i = 1, 4, 6, 7, 9$ and 13) both while cooling and heating. The measured frequency shifts of these modes are plotted in figure 4. The frequencies of the

Table 3. The ρv^2 as a function of elastic constant in the hexagonal (6mm) and orthorhombic (mm2) phases.

Phonon	Mode		6mm	mm2
[100]	L*	γ_1	c_{11}	c_{11}
	T	γ_2	$\frac{1}{2}(c_{11}-c_{12})$	c_{66}
	T	γ_3	c_{44}	c_{55}
[010]	L*	γ_4	c_{11}	c_{22}
	T	γ_5	c_{44}	c_{44}
	T*	γ_6	$\frac{1}{2}(c_{11}-c_{12})$	c_{66}
[001]	L*	γ_7	c_{33}	c_{33}
	T	γ_8	c_{44}	c_{55}
	T*	γ_9	c_{44}	c_{44}
[110]	L	γ_{10}	c_{11}	$\frac{1}{4}\{c_{11}+c_{22}+2c_{66}+[(c_{22}-c_{11})^2+4(c_{12}+c_{66})^2]^{1/2}\}$
	T	γ_{11}	$\frac{1}{2}(c_{11}-c_{12})$	$\frac{1}{4}\{c_{11}+c_{22}+2c_{66}-[(c_{22}-c_{11})^2+4(c_{12}+c_{66})^2]^{1/2}\}$
	T	γ_{12}	c_{44}	$\frac{1}{2}(c_{44}+c_{55})$
[011]	L*	γ_{13}	$\frac{1}{4}\{c_{11}+c_{33}+2c_{44}+[(c_{33}-c_{11})^2+4(c_{13}+c_{44})^2]^{1/2}\}$	$\frac{1}{4}\{c_{22}+c_{33}+2c_{44}+[(c_{33}-c_{22})^2+4(c_{23}+c_{44})^2]^{1/2}\}$
	T	γ_{14}	$\frac{1}{4}\{c_{11}+c_{33}+2c_{44}-[(c_{33}-c_{11})^2+4(c_{13}+c_{44})^2]^{1/2}\}$	$\frac{1}{4}\{c_{22}+c_{33}+2c_{44}-[(c_{33}-c_{22})^2+4(c_{23}+c_{44})^2]^{1/2}\}$
	T	γ_{15}	$\frac{1}{2}(c_{44}+c_{11}-c_{12})$	$\frac{1}{2}(c_{55}+c_{66})$
[101]	L	γ_{16}	$\frac{1}{4}\{c_{11}+c_{33}+2c_{44}+[(c_{33}-c_{11})^2+4(c_{13}+c_{44})^2]^{1/2}\}$	$\frac{1}{4}\{c_{11}+c_{33}+2c_{55}+[(c_{33}-c_{11})^2+4(c_{13}+c_{55})^2]^{1/2}\}$
	T	γ_{17}	$\frac{1}{4}\{c_{11}+c_{33}+2c_{44}-[(c_{33}-c_{11})^2+4(c_{13}+c_{44})^2]^{1/2}\}$	$\frac{1}{4}\{c_{11}+c_{33}+2c_{55}-[(c_{33}-c_{11})^2+4(c_{13}+c_{55})^2]^{1/2}\}$
	T	γ_{18}	$\frac{1}{2}(c_{44}+c_{11}-c_{12})$	$\frac{1}{2}(c_{44}+c_{66})$

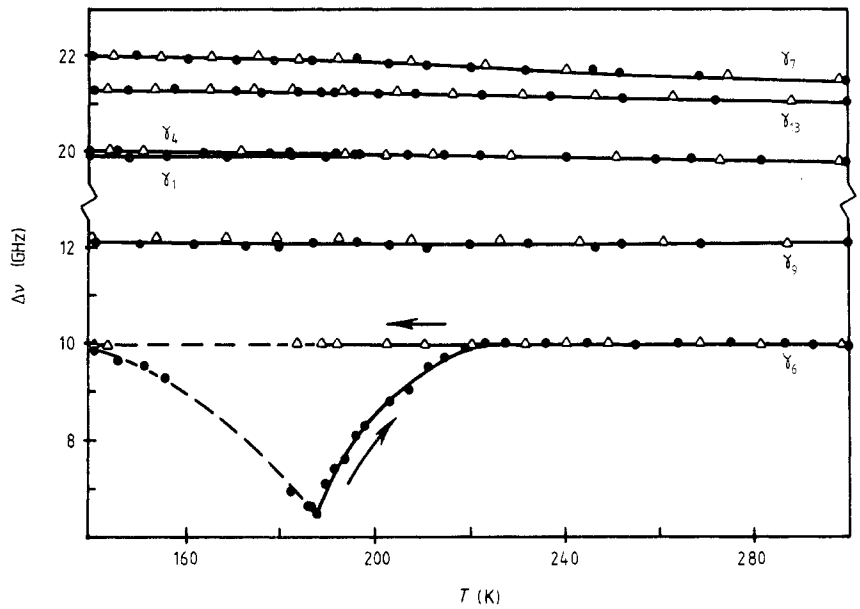

Figure 4. Temperature dependences of the Brillouin shifts $\Delta\nu$.

longitudinal modes γ_1, γ_4, γ_7 and γ_{13} are slightly temperature-dependent: they increase with temperature up to T_5, but remain constant above T_5. All these lines show the same behaviour on cooling and heating. The transverse mode γ_9 corresponding to the c_{44} elastic constant (see table 3) was found to be temperature-independent. However, the frequency shifts were slightly lower while heating, especially in the low-temperature phase. The 6mm → mm2 transition is associated with acoustic phonon softening related to the transverse mode $c_{66} = \frac{1}{2}(c_{11} - c_{22})$ [15, 45]. In fact, the γ_6 mode was found to be strongly temperature-dependent while heating. The frequency shift of this mode increases slowly from 9.87 GHz at 300 K to 10.02 GHz at 223 K and then falls to 6.48 GHz at 188.4 K. Because of the low signal-to-noise ratio below T_5 we could not observe the γ_6 mode in the entire temperature region studied. The broken lines in the plot of $\gamma_6(T)$ indicate regions of extremely weak scattering.

The temperature dependences of elastic constants as calculated from Brillouin shifts are plotted in figure 5. The c_{11} and c_{33} elastic constants increase linearly with decreasing temperature and their temperature dependences may be described as: $c_{11} = 5.800 - 0.001(T - T_5)$ and $c_{33} = 6.950 - 0.002(T - T_5)$ (in units of 10^{10} N m^{-2}). The c_{44} elastic constant is essentially temperature-independent within experimental accuracy. The sound velocity related to the c_{66} constant changes from 2440 m s^{-1} at 300 K to 1600 m s^{-1} at T_5 (=188.4 K). The values of the c_{23} elastic constant were calculated using the expression of ρv^2 for the γ_{13} mode given in table 3.

The above results have been obtained using several samples cut from three different single crystals of $LiKSO_4$ and were very reproducible except for one experiment where we observed the two longitudinal modes simultaneously for the [0 1 0] phonon (see figure 6). Similar behaviour of the longitudinal modes was reported by Ganot *et al* [23]. The first component corresponds to the values of c_{11} in figure 5, while the second one (c'_{11}) was found to be lower by about 20%. After holding the sample at constant temperature (174 K) for several hours the spectrum became 'normal' again and developed only one longitudinal component. Because of sample cracking at 164 K we were not able to repeat

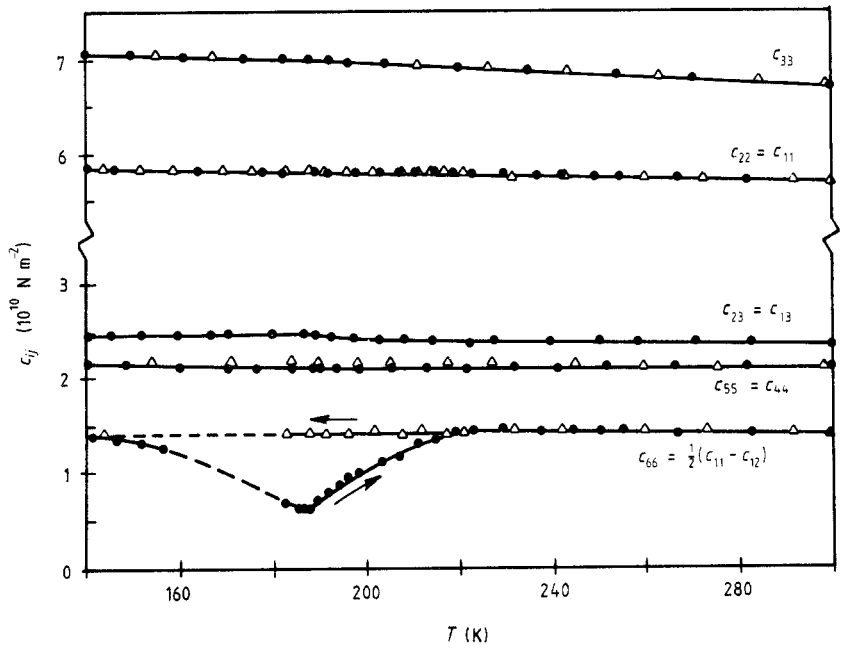

Figure 5. Temperature dependences of the elastic constants c_{ij}.

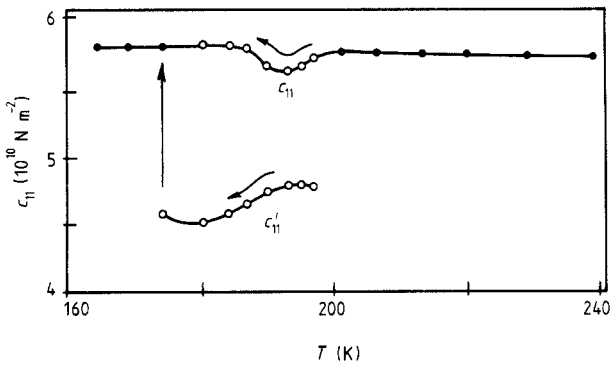

Figure 6. The c_{11} elastic constant versus temperature; the open circles indicate the region of temperatures where two longitudinal components were simultaneously observed.

this measurement on heating. The effect mentioned above may be due to the existence of a mixed-phase region in the sample (and was reported earlier by Tomaszewski and Lukaszewicz [47]). Finally, in table 4 we compare our elastic constants with those previously obtained by various Brillouin scattering experiments on $LiKSO_4$. It should be emphasised, however, that the present study is the most complete to date and earlier analyses of the elastic properties of $LiKSO_4$ as noted above were rather fragmentary.

3. Theory

Recently, An *et al* [3] presented a brief outline of the Landau free-energy expansion for $LiKSO_4$ in the vicinity of the PIV $\rightarrow$ PV transition, i.e. around T_4. Their free energy

Table 4. Comparison of elastic constants (in units of 10^{10} N m^{-2}) of $LiKSO_4$ obtained in the course of various Brillouin scattering experiments (300 K).

Authors	c_{11}	c_{33}	c_{44}	c_{66}	c_{12}	c_{13}
Pimeta *et al* [38]	5.74	6.73	2.11	1.42	2.92	—
Ganot *et al* [23]	5.62	6.63	—	—	—	—
Ganot *et al* [22][a]	5.69	6.67	1.86	2.00[b]	—	2.65
Present experiment	5.67	6.71 ± 0.08	2.14	1.42 ± 0.05	2.83 ± 0.15	2.35

[a] At 293 K.
[b] Has a large uncertainty.

involved the order parameter Q, which transforms according to an irreducible representation of the point group 6 and all the strain components e_i. It did not, however, include polarisation P, which is visibly affected at the transition [21]. Furthermore, another recent paper [49] was devoted to a Landau theory description of the PV → PVI transition taking place at T_5. The assumption was that spontaneous strain, i.e. $e_s \equiv (e_{xx} - e_{yy})/\sqrt{2}$, was the primary order parameter and the expansion also involved polarisation. We shall base our theoretical analysis on these two papers for several reasons. First, the two transitions are rather close together, especially when hysteresis effects are included, and hence they should be covered by a single free-energy expansion with respect to the prototypic phase 6. Secondly, the sequence of transitions adopted by these authors coincides with our opinion on that matter, i.e. that it is $6 \underset{T_4}{\longrightarrow} 6mm \underset{T_5}{\longrightarrow} mm2$. It is also noteworthy that 6mm is a subgroup of both mm2 and 6 and all the groups are polar. Compared with the previous theoretical models [3, 49], we shall make some changes and adjustments called for by the recent experimental results. First of all, since in this temperature range $LiKSO_4$ is an improper ferroelectric, polarisation must be consistently included in the study. We also believe that the PV → PVI transition is a pseudo-ferroelastic transition involving an order parameter η, which transforms according to the E_2 representation of 6mm, but η differs from e_s. The reason for this statement is drawn from the incomplete softening of c_{2s} and the simultaneous metastability of the paraelastic phase, as shown in figure 5. We have attempted free-energy modelling with e_s being the primary order parameter, but in the course of study it became clear to us that such an assumption would lead to serious difficulties in explaining the various hysteretic effects seen in the experiment.

The Landau-type free-energy expansion [30] that we postulate for this sequence of transitions is

$$F = F_1(Q) + F_2(P) + F_3(\eta) + F_4(e_s, e_i) + F_{12}(Q, P) + F_{14}(Q, e_i, e_s) + F_{34}(\eta, e_s, e_i) + F_{234}(P, \eta, e_s) \tag{4}$$

where, in accordance with the symmetry principles at play, the various contributions are written as follows. The primary order parameter term for the upper transition at T_4 is

$$F_1(Q) = (A_2/2)Q^2 + (A_4/4)Q^4 + (A_6/6)Q^6 \tag{5}$$

where $A_2 = a(T - T_4^0)$, $A_4 < 0$ and $A_6 > 0$. The polarisation term is

$$F_2(P) = (B_2/2)P^2 + (B_4/4)P^4 \tag{6}$$

where $B_2 > 0$ and $B_4 > 0$, so that polarisation does not experience spontaneous symmetry breaking by itself. The primary order parameter term for the lower transition is

$$F_3(\eta) = (\alpha_0/2)\eta^2 + (\beta_0/3)\eta^3 + (\gamma_0/4)\eta^4 \tag{7}$$

where $\alpha_0 = \alpha'(T - T_5^0)$, $\gamma_0 > 0$ and the sign of β_0 is not known *a priori*, but according to the microscopic considerations of Zeks *et al* [49], $\beta_0 < 0$. The elastic term is

$$F_4(e_s, e_i) = \tfrac{1}{2}c_{2s}^0 e_s^2 + \tfrac{1}{2}\sum_{i,j(\neq s)} c_{ij}^0 e_i e_j + \sum_{i(\neq s)} c_{is}^0 e_i e_s \tag{8}$$

which is a typical second-order expansion with respect to the elastic degrees of freedom [45] and all the coupling coefficients are assumed nearly constant in the temperature range considered according to our assumption about the pseudo-ferroelastic nature of the transition. Then, the interaction energies are assumed in the lowest order of approximation as

$$F_{12}(Q, P) = \nu QP \tag{9}$$

$$F_{14}(Q, e_s, e_i) = \tfrac{1}{2}\left(K_s e_s Q^2 + \sum_{i(\neq s)} K_i e_i Q^2 + \tau_s e_s^2 Q^2 + \sum_{i(\neq s)} \tau_i e_i^2 Q^2\right) \tag{10}$$

$$F_{34}(\eta, e_s, e_i) = \mu e_s \eta + \tfrac{1}{2}\sum_{i(\neq s)} \lambda_i e_i \eta^2 + \tfrac{1}{2}\sum_{i(\neq s)} \rho_i e_i^2 \eta^2 \tag{11}$$

$$F_{234}(P, \eta, e_s) = \xi_1 \eta^2 P + \xi_2 e_s^2 P \tag{12}$$

where the summations in equations (10) and (11) run over all strain indices different from spontaneous strain and which are non-zero by symmetry principles within a given phase. The various coupling coefficients K_i, τ_i, λ_i and ρ_i are *a priori* all different unless specific symmetry conditions apply for the given phase.

It is assumed that the first-order expansion terms, i.e. $F_1 + F_2 + F_3 + F_4$, are dominant to the extent of determining the transition temperatures, especially on approaching them from above since the interaction terms involve quantities of smaller orders of magnitude there. Consequently, it is found that $T_4 = T_4^0 + A_4^2/4aA_6$ with the region of coexistence of the disordered $Q_0(6)$ and ordered $Q_\pm(6mm)$ phases between T_4^0 and $T_4^s \equiv T_4^0 + A_4^2/3aA_6$. This roughly (since we neglected couplings here) corresponds to the extent of the thermal hysteresis. Hence, we deduce that $A_4^2/3aA_6 \simeq (40\text{–}50)$ K. A typical plot of Q in such a case is shown in figure 7. The discontinuity in Q at T_4 equals: $\Delta Q = (-A_4/A_6)^{1/2}$.

Minimisation of the free energy (equation (4)) with respect to all its thermodynamic variables results in a set of five coupled non-linear algebraic equations, which are very difficult to analyse exactly. However, certain approximations will give us very important information about the system. Above T_4, $\eta = 0$ and also, assuming negligible influence of e_s on P, we find a relationship between P and Q:

$$Q \simeq -(1/\nu)(B_2 P + B_4 P^3). \tag{13}$$

From equation (13) we readily find that the effective polarisation energy of the sample may, as a result of coupling with Q, exhibit symmetry breaking. In order for it to agree with experiment, which predicts the transition to produce a continuous change in polarisation, we expect that close to T_4: $B_2 \simeq 4A_6\nu^2/A_4^2$ and $B_2 B_4 A_4^2/4A_6\nu^2 + A_4 B_2^4/4\nu^4 - 3B_4/4 > 0$. Below T_4, we may decouple P from Q and replace it with an effective 'molecular' field $E_{\text{eff}}(T)$ so that

$$F_2 + F_{12} \simeq \tfrac{1}{2}\chi^{-1}P^2 - E_{\text{eff}}(T)P \tag{14}$$

and, above T_5, polarisation is given by $P = P_s(T) = \chi E_{\text{eff}}(T)$, where $P_s(T)$ corresponds to the measured values [21].

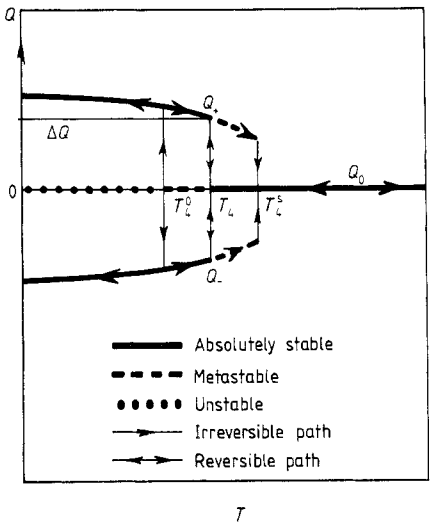

Figure 7. A typical plot of Q for the PIV → PV transition.

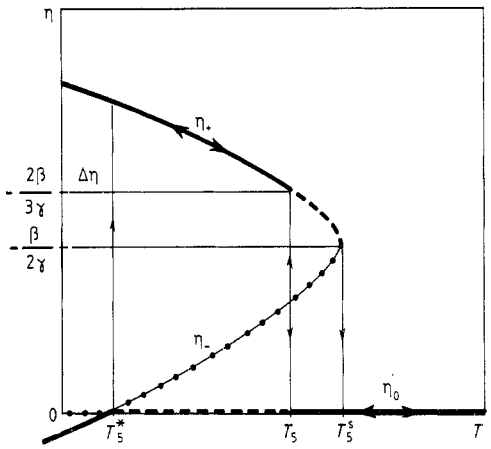

Figure 8. A typical plot of η for PV → PVI transition. (Key as for figure 7).

While polarisation undergoes continuous change at T_4, the strain tensor's components experience discontinuities (as found experimentally by Tomaszewski and Lukaszewicz [46]), namely

$$\Delta e_s \simeq -K_s(\Delta Q)^2/2[c_{2s}^0 + \tau_s(\Delta Q)^2] \tag{15}$$

and

$$\Delta e_i \simeq -K_i(\Delta Q)^2 \Big/ 2\Big(1 + \sum_{j(\neq s)} s_{ij}^0 \tau_i (\Delta Q)^2\Big) \tag{16}$$

where s_{ij}^0 is the compliance tensor. This, then, is expected to distort the prototypic 6 structure in such a way as to produce the 6mm (intermediate) structure. As discussed earlier, the transition may or may not materialise in all the parts of the sample at the same time and temperature, leading to complicated experimental results. Also, in the vicinity of T_4 the elastic constants are found as

$$c_{2s} \equiv \partial^2 F/\partial e_s^2 = c_{2s}^0 + \tau_s Q^2 + \xi_2 P \tag{17}$$

$$c_{ij} \equiv \partial^2 F/\partial e_i \partial e_j = \tfrac{1}{2} c_{ij}^0 \tag{18}$$

$$c_{is} \equiv \partial^2 F/\partial e_i \partial e_s = c_{is}^0 \tag{19}$$

$$c_{ii} \equiv \partial^2 F/\partial e_i^2 = c_{ii}^0 + \tau_i Q^2. \tag{20}$$

Hence, only c_{2s} and c_{ii} may experience a discontinuity at T_4. This, in fact, is borne out by experiment [3, 23, 36], which indicates that c_{2s} jumps by approximately 17% ($=\tau_s(\Delta Q)^2/c_{2s}^0$), c_{11} by about 20% ($=\tau_1(\Delta Q)^2/c_{11}^0$) and c_{33} by a very small but noticeable amount. Furthermore, all the quantities that depend on Q, i.e. e_s, e_i, c_{2s} and c_{ii}, should exhibit hysteretic behaviour.

As we approach T_5 from above, we are interested in the deviations of e_s and e_i from their 6mm-values rather than the 6-values, which was the case around T_4. Therefore, we effectively replace $F_1 + F_4 + F_{14}$ by a new expression, namely

$$F_1 + F_4 + F_{14} \simeq \tfrac{1}{2}c_{2s}^0 e_s^2 - \sigma_s^{\text{eff}}(T)e_s + \tfrac{1}{2}\sum_{i,j(\neq s)} c_{ij}^0 e_i e_j - \sigma_i^{\text{eff}}(T)e_i + c_{is}^0 e_i e_s \tag{21}$$

where e_s and e_i determine these deviations from the 6mm-values and where σ_s^{eff} and σ_i^{eff} are the effective stresses required to reproduce the temperature dependence of e_s and e_i, respectively, as a result of their coupling to Q. This approximation greatly simplifies an otherwise very difficult analysis in the vicinity of T_5.

The transition temperature is approximately determined using F_3 of equation (7), $F_2 + F_{12}$ of equation (14) and the coupling between η and P as given by equation (12). Expanding $P_s(T)$ in a power series in the neighbourhood of T_4^0 and keeping only a linear term yields

$$P_s(T) \simeq P_0 + p_1(T - T_4^0). \tag{22}$$

From figure 1 of [36], we find that $T_4^0 \simeq 200$ K and $p_1 = 0.2 \times 10^{-4}$ C K^{-1} m^{-2}. In fact the experiment did not measure P_0 but only the change $\Delta P_s \equiv |P - P_0|$. With this substituted back into F, an effective free energy for the order parameter η can be written as

$$F_5^{\text{eff}}(\eta) \simeq (\alpha/2)\eta^2 + (\beta/3)\eta^3 + (\gamma/4)\eta^4 \tag{23}$$

where the new coefficients are $\alpha = \alpha_0 + 2\xi_1 P_s(T)$, $\beta = \beta_0$ and $\gamma = \gamma_0 - 2\chi\xi^2$. This effective free energy is then subject to minimisation with respect to η, which results in three solutions: $\eta_0 = 0$ and $\eta_\pm = [-\beta \pm (\beta^2 - 4\alpha\gamma)^{1/2}]/2\gamma$. Denoting $T_4^* \equiv T_4^0 - 2\xi P_0/(\alpha' + 2\xi p_1)$ and $\alpha^* = \alpha' + 2\xi p_1$ so that $\alpha = \alpha^*(T - T_4^*)$, gives the plot of $\eta(T)$ for $\beta < 0$ as shown in figure 8. The case of $\beta > 0$ can be obtained by replacing η with $-\eta$ and interchanging the '+' and the '−' labels. Thus, the first-order transition takes place at $T_5 = T_5^* + 2\beta^2/9\alpha^*\gamma$, where the order parameter experiences a discontinuity $|\Delta\eta| = |2\beta/3\gamma|$. The ordered phase is stable below $T_5^s \equiv T_5^* + \beta^2/4\alpha^*\gamma$ and the disordered phase is stable above T_5^*. Experimental results estimate the amount of hysteresis at between 50 and 120 K (which should be equal to $\beta^2/4a^*\gamma$). The other ordered phase becomes metastable below T_5^*. Therefore, there is a range of coexistence of the ordered and disordered phases between T_5^* and T_5^s.

The temperature dependence of polarisation can be found by minimising the free energy with respect to P as

$$P \simeq P_s(T) - \chi(\xi_1\eta^2 + \xi_2 e_s^2) \tag{24}$$

so that with $\xi_1 > 0$ and $\xi_2 > 0$ there is a drop (as observed) in P at T_5. In fact, experiment shows that, at T_5, $\Delta P \simeq 20 \times 10^{-4}$ C m^{-2} [12] and $\Delta\varepsilon \simeq 8 \times 10^{-3}$ [47]. We have plotted $P(T)$ in figure 9 following Breczewski *et al* [12], which is compared to the theroretical prediction based on equation (24) and the form of $\eta(T)$. Minimisation of the free energy with respect to strain components yields

$$e_s \simeq [\sigma_{\text{eff}}(T) - \mu\eta]/(c_{2s}^0 + 2\xi_2 P) \tag{25}$$

and

$$e_i \simeq -\sum_j s_{ij}^0(c_{is}^0 e_s + \tfrac{1}{2}\lambda_i\eta^2). \tag{26}$$

Thus, both of them, and especially e_s, should exhibit a discontinuity at T_5 and hysteresis effects due to $\eta(T)$.

Finally, the second-order elastic coefficients are found in the usual way as

$$c_{2s} = c_{2s}^0 + 2\xi_2 P \qquad \text{for } e_s \neq 0 \tag{27a}$$

$$c_{2s} = c_{2s}^0 \qquad \text{for } e_s = 0 \tag{27b}$$

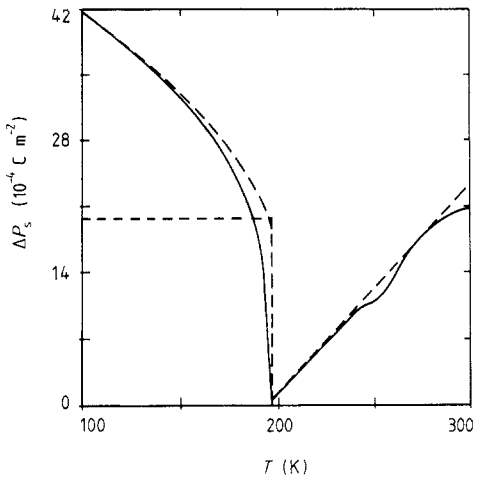

Figure 9. Experimental (——) and theoretical (- - - -) plots of the temperature dependence of spontaneous polarisation.

and

$$c_{ij} = c_{ij}^0 \qquad c_{is} = c_{is}^0 \tag{28}$$

$$c_{ii} = c_{ii}^0 + \rho_i \eta^2. \tag{29}$$

Thus, once again, only the diagonal ones (c_{2s} and c_{ii}) are expected to have a pronounced temperature dependence, which indeed has been confirmed experimentally. We have made a quadratic fit to c_{2s} above T_5 and below T_5, which gives

$$c_{2s} = [0.64 + 4.04 \times 10^{-2}(T - T_5) - 4.84 \times 10^{-4}(T - T_5)^2] \times 10^{10}\ \mathrm{N\,m^{-2}} \tag{30a}$$

for $T > T_5$ (valid up to 43 K above T_5), and

$$c_{2s} = [0.58 + 2.87 \times 10^{-2}(T_5 - T) - 2.35 \times 10^{-4}(T_5 - T)^2] \times 10^{10}\ \mathrm{N\,m^{-2}} \tag{30b}$$

for $T < T_5$ (valid up to 48 K above T_5). In particular, it is quite remarkable that the plot of c_{2s} (figure 5) and that of P (figure 9) looks very similar with respect to the dip at the transition temperature. This is in agreement with our equation (27*a*), which indicates that c_{2s} should be proportional to P. We have also determined that c_{2s} for the ferroelastic phase and P are strongly correlated on both sides of T_5. In fact, using the values at T_5 we can calculate the coupling constant $\xi_2 = \Delta c_{2s}/2\Delta P \simeq +1.8 \times 10^{12}\ \mathrm{N\,C^{-1}}$. The other interesting feature is the metastability of the disordered phase (6mm) down to at least 140 K, which can be explained by a lack of coupling between $\varepsilon = 0$ and $P = 0$.

More detailed analyses of these transitions will be possible once the order parameters Q and η are unambiguously identified and their physical properties are found. This would enable fits of experimental data to the model free energy of equation (4). However, even at this preliminary stage of theoretical modelling there appears to be a significant amount of qualitative agreement with experiment.

4. Conclusions

In this paper we have reported Brillouin scattering results for $LiKSO_4$ in the range of temperatures between 140 and 300 K. Based on the temperature dependence of the longitudinal and transverse Brillouin modes, we have calculated all the non-zero components of the elastic stiffness tensor. The results obtained generally agree with those

of other measurements using various experimental techniques (Brillouin scattering, pyroelectric studies, x-ray and neutron scattering). The most interesting experimental observation was that the c_{66} constant exhibited a thermal hysteresis effect with a persistence of the para-elastic phase throughout the above temperature range. We have also presented a (possible) theoretical account of the observed phenomena and made some predictions, which could be verified by future investigations, most notably that the PV $\rightarrow$ PVI transition is of a pseudo-ferroelastic type. The theoretical model is based on a Landau expansion of the free energy involving coupling between two separate order parameters for the two transitions at T_4 and T_5 on the one hand, and spontaneous polarisation and spontaneous strain on the other. This is crucial to further comparisons with experimental data. We have subsequently performed standard minimisation analyses using some additional approximations, such as the molecular-field approximation, in order to provide relatively simple answers. The results obtained within this model are consistent with several sets of hitherto unexplained experimental data, such as the temperature behaviours of spontaneous polarisation and the c_{2s} elastic coefficient and discontinuities of other second-order elastic coefficients and strain components.

In our analysis we have assumed that the two transitions at T_4 and T_5 are rather well separated, which may not always be the case. Taking into account the hysteresis effects present in both cases may lead to complications since the intervals (T_4^*, T_4^s) and (T_5^0, T_5^s) may overlap or at least come very close to each other. If this happens, then both η and Q should be retained in the expansion, leading to rather complicated minimisations and a possibility of new phases or transient behaviours.

Obviously, other possible explanations should also be seriously considered. If, for example, phase PV is not 6mm but 3m then the PV $\rightarrow$ PVI transition would have to involve a two-component order parameter. It is also conceivable that fluctuations of spontaneous polarisation play an important role [32, 40, 41]. They may be coupled to spontaneous strain and stress and lead to an incomplete softening of c_{2s}.

Acknowledgments

This research has been supported by grants awarded by the Natural Sciences and Engineering Research Council of Canada to JAT, HK and MJC. One of the authors (BM) would like to express his gratitude to the faculty and staff of the Department of Physics at Memorial University of Newfoundland during his stay in St John's.

References

[1] Abello L, Chhor K and Pommier C 1985 *J. Chem. Thermodyn.* **17** 1023
[2] Ahmad S F, Kiefte H, Clouter M J and Whitmore M D 1982 *Phys. Rev.* B **26** 4239
[3] An T, Ling-qing L, Ben-yuen G, Yu-jun M, Hua-quang Y and Yan-yun W 1987 *Solid State Commun.* **61** 1
[4] Ando T 1962 *J. Phys. Soc. Japan* **17** 937
[5] Balagurov A M Mróz B, Popa N C and Savenko B N 1986 *Phys. Status Solidi* **96** 25
[6] Balagurov A M, Savenko B N, Dlouhá M, Vratislav S and Jirák Z 1984 *Phys. Status Solidi* a **83** K117
[7] Bansal M L, Deb S K, Roy A P and Sahni V C 1980 *Solid State Commun.* **36** 1047
[8] Bansal M L and Roy A P 1984 *Phys. Rev.* B **30** 7307
[9] Bhakay-Tamhane S, Sequeira A and Chidambaram R 1985 *Solid State Commun.* **53** 197
[10] Blittersdorf H 1928 *Z. Kristallogr.* **67** 279
[11] Bradley A J 1925 *Phil. Mag.* **49** 1225

[12] Breczewski T, Krajewski T and Mróz B 1981 *Ferroelectrics* **33** 9
[13] Cach R, Tomaszewski P, Bastic P and Bornarel J 1984 *Ferroelectrics* **53** 337
[14] Cach R, Tomaszewski P E and Bornarel J 1985 *J. Phys. C: Solid State Phys.* **18** 915
[15] Cowley R A 1976 *Phys. Rev.* B **13** 4877
[16] Drozdowski M, Holuj F and Czajkowski M 1983 *Solid State Commun.* **45** 1005
[17] Errandonea G 1980 *Phys. Rev.* B **21** 5221
[18] Filho J M, Moreira J E, Melo F E A, Germano F A and Sombra A S B 1986 *Solid State Commun.* **60** 189
[19] Fischmeister H F and Roennquist A 1960 *Arkiv. Chem.* **15** 393
[20] Fonseca C H A, Ribeiro G M, Gazzinelli R and Chaves A S 1983 *Solid State Commun.* **46** 221
[21] Fujimoto S, Yasuda N, Hibino H and Narayanan P S 1984 *J. Phys. D: Appl. Phys.* **17** L35
[22] Ganot F, Kihal B, Dugautier C, Farhi R and Moch P 1987 *J. Phys. C: Solid State Phys.* **20** 4491
[23] Ganot F, Kihal B, Farhi R and Moch P 1985 *Japan. J. Appl. Phys.* **24** 491 Suppl. 24-2
[24] Hiraishi J, Taniguchi N and Takahashi H 1976 *J. Chem. Phys.* **65** 3821
[25] Holuj F and Drozdowski M 1981 *Ferroelectrics* **36** 379
[26] Ivanov N R 1985 *Ferroelectrics* **64** 329
[27] Karppinen M, Lundgren J-O and Liminga R 1983 *Acta Crystallogr.* C **39** 34
[28] Krajewski T, Breczewski T, Kassem M and Mróz B 1984 *Ferroelectrics* **55** 143
[29] Krajewski T, Breczewski T, Piskunowicz P and Mróz B 1985 *Ferroelectrics Lett.* **4** 95
[30] Landau L D and Lifshitz E M 1958 *Statistical Physics* (London: Pergamon)
[31] —— 1959 *Theory of Elasticity* (New York: Addison Wesley)
[32] Lüthy B and Rehwald W 1981 *Structural Phase Transitions I* ed. K A Müller and H Thomas (New York: Springer)
[33] Maezawa K, Takeuchi H and Ohi H 1985 *J. Phys. Soc. Japan* **54** 3106
[34] Meng Q-A and Cao A-J 1982 *Acta Phys. Sinica* **31** 1405
[35] Mróz B, Kiefte H, Clouter M J and Tuszyński J A 1987 *Phys. Rev.* B **36** 3745
[36] Mróz B, Krajewski T, Breczewski T, Chomka W and Sematowicz D 1982 *Ferroelectrics* **42** 459
[37] Murthy K and Bhat S V 1988 *J. Phys. C: Solid State Phys.* **21** 597
[38] Pimeta M A, Luspin Y and Hauret G 1986 *Solid State Commun.* **59** 481
[39] Prasad T R, Venudhar Y C, Iyengar L and Rao K V K 1978 *Pramana* **11** 81
[40] Pytte E 1971 *Structural Phase Transitions and Soft Modes* ed. E J Samuelsen, E Andersen and J Feder (Oslo: Universitets Forlaget)
[41] Rehwald W 1973 *Adv. Phys.* **22** 721
[42] Sandomirski P A, Meshalkin S S and Rozhdestvenskaya I V 1983 *Kristallografiya.* **28** 67
[43] Sharma D P 1979 *Pramana* **13** 223
[44] Teeters D and French R 1982 *Phys. Rev.* B **26** 5897
[45] Toledano P, Fejer M M and Auld B A 1983 *Phys. Rev.* B **27** 5717
[46] Tomaszewski P E and Lukaszewicz K 1982 *Phys. Status Solidi* a **71** K53
[47] —— 1983 *Phase Transitions* **4** 37
[48] Young P W, Katiyar R S and Scott J F 1984 *J. Raman Spectrosc.* **15** 347
[49] Zeks B, Lavrencic B B and Blinc R 1984 *Phys. Status Solidi* b **122** 399